Hindawi
Mathematical Problems in Engineering
Volume 2022, Article ID 6279498, 16 pages
https://doi.org/10.1155/2022/6279498

Research Article

Effect of Diffusion-Thermo on MHD Flow of a Jeffrey Fluid Past an Exponentially Accelerated Vertical Plate with Chemical Reaction and Heat Generation

Ahmad Shafique,[1] Zaib Un Nisa,[2] Muhammad Imran Asjad,[3] Mudassar Nazar,[1,4] and Fahd Jarad[5,6,7]

[1]*Centre for Advanced Studies in Pure and Applied Mathematics, Bahauddin Zakariya University, Multan, Pakistan*
[2]*Department of Mathematics, University of Education Lahore Multan Campus, Multan, Pakistan*
[3]*Department of Mathematics, University of Management and Technology Lahore 54770, Pakistan*
[4]*School of Mathematical Sciences, University of Science and Technology of China, Hefei, Anhui, China*
[5]*Department of Mathematics, Cankaya University, 06790 Etimesgut, Ankara, Turkey*
[6]*Department of Mathematics, King Abdulaziz University, Saudi Arabia*
[7]*Department of Medical Research, China Medical University, Taichung 40402, Taiwan*

Correspondence should be addressed to Fahd Jarad; fahd@cankaya.edu.tr

Received 10 January 2022; Accepted 19 February 2022; Published 24 May 2022

Academic Editor: Arshad Riaz

In many flow phenomenons of fluid with medium molecular weight, the energy flux is effected due to the inhomogeneity of concentration of mass. This contribution of the concentration to the energy flux is considered as diffusion-thermo effect or Dufour effect. In this research article the diffusion-thermo effect is addressed for the magnetohydrodynamics (MHD) flow of Jeffrey's fractional fluid past an exponentially accelerated vertical plate with generalized thermal and mass transports through a porous medium. For the generalization of the thermal and mass fluxes the constant proportional Caputo (CPC) fractional derivative is utilized. The governing of this generalized flow are reduced to non-dimensional forms and then solved semi analytically by Laplace transform. In additions the physical aspects of flow and material parameters especially the effect of *Du* and fractional parameters are discussed by sketching the graphs. From the graphical illustration, it is concluded that in the presence of Dufour effect flow speeds up. Moreover, a comparison between fractionalized and ordinary velocity fields is also drawn and it is also observed that fractional model with constant proportional derivative is of the more decaying nature as compare to the model contracted with classical Caputo and Caputo fractional derivatives.

1. Introduction

The non-Newtonian fluids posses the diverse nature from Newtonian fluids due to their complex rheological properties. Now a days the study of non-Newtonian becomes a popular research area due to its scientific and technological applications in the processing industry, and biological sciences, like making of plastic sheets, lubricant's performance and motion of biological fluid. There are several non-Newtonian fluid models have been presented to demonstrate the distinction between Newtonian and non-Newtonian fluids but the Jeffrey fluid model is more efficient to demonstrate attribute of stress relaxation for memory time scale (the relaxation of time). Mohd-Zin et al. [1] studied the porosity effect on unsteady MHD free convection flow of Jeffrey fluid past an oscillating vertical plate with ramped wall temperature. Bajwa et al. [2] solved a problem of transient flow of Jeffrey fluid semi-analytically over permeable wall. Asgir et al. [3] discussed the heat transfer analysis of channel flow of MHD Jeffrey fluid with porosity.

The model on Jeffrey fluid be simplest and most popular. Some of the work on Jeffrey fluid are of Das [4] and Qasim [5]. Ali et al. [6] discussed the magnetohydrodynamic fluctuating free convection flow of incompressible electrically conducting viscoelastic fluid in a porous medium in the presence of a pressure gradient. Shah et al. [7] worked on the new semi analytical technique for the solution of fractional Order Navier Stokes equation.

The fractional derivative is the generalization of ordinary derivative by taking the non-integer order of differentiation. Due its generalized property the fractional derivative becomes a potent tool to describe the heat and mass transfer phenomenons and has attained the attention by researchers. Chandra [8] present the MHD flow for Jeffrey fluid past an inclined porous plate by applying Laplace transform method. Jameel et al. [9] obtain the analytic solutions for the incompressible unsteady flow of fractionalized MHD Jeffrey fluid over an accelerating porous plate with linear slip effect by using Caputo fractional derivative. Abro et al. [10] obtain the solution of Jeffrey fluid flow acquired by non-singular kernel (Caputo-Fabrizio) using integral transform technique. During the last decade, different generalized fractional derivatives have appeared in the literature that are derivatives of Caputo, Caputo-Fabrizio, Atangana-Baleanu [11, 12]. Jawad et al. [13] observed the behavior of Caputo time fractional model based on generalized Fourier's and Fick's laws for Jeffrey Nano fluid. Siddique et al. [14] studied the unsteady double convection flow of a magnetohydrodynamics (MHD) differential-type fluid flow in the presence of Dufour effect, Newtonian heating, and heat source over an infinite vertical plate with fractional mass diffusion and thermal transports.

Sandeep et al. [15] discussed the behavior of momentum and heat transfer on Jeffrey, Maxwell and Oldroyd-B nanofluids over a stretching surface in the presence of transverse magnetic field, non-uniform heat source/sink. A magnetohydrodynamic Jeffrey fluid flow with thermal and mass transfer on an infinitely rotating upright cone investigated by Saleem et al. [16]. Sulochana et al. [17] solved a problem of a MHD radiative Casson fluid flow numerically over a wedge to analyze the heat and molecular transfer. A bio convective nanoliquid flow with the effect of second order slip and chemical reaction between the parallel plates studied by Acharya et al. [18]. The radiative couple stress fluid and chemically reactive nanofluid over a stretched cylinder with magnetic effect analyzed by Acharya et al. [19, 20]. Riaz et al. [21] obtained the solution of peristaltic flow of Prandtl fluid by using homotopy perturbation method. The role of hybrid nanoparticles in thermal performance of peristaltic flow of Eyring-Powell fluid model have discussed by Riaz et al. [22].

Different types of fractional operators has discussed by Yuri-Luchko [23]. Baleanu et al. [24] presented a new fractional operator combining proportional Caputo and solve different kind of example with CPC derivative. Chu et al. [25] worked on fractional model of Second grade fluid induced by generalized thermal and molecular fluxes with constant proportional Caputo. Siddique et al. [26] analyzed the blood liquor model fractionalized with constant proportional Caputo fractional derivative and Dolat et al. [27] investigate a fractional model of MHD viscous fluid with heat transfer by using the constant proportional Caputo fractional derivative.

The purpose of this article is to utilized the Constant proportional Caputo fractional derivative for the investigation of diffusion-thermo effect on MHD flow of Jeffrey fluid past an exponentially accelerated vertical plate in the presence of chemical reaction, and heat generation through a porous medium with generalized heat and mass fluxes. Constant proportional Caputo fractional derivative is considered for the generalization of constitutive equations for heat and mass fluxes. Initially, the proposed governing equations are reduced to non-dimensional form then solved semi analytically via Laplace transform. The physical aspects of flow regarding involved parameters are also discussed by sketching some graphs for velocity field of Jeffrey fluid. Moreover the obtained result for velocity with CPC will compare with ordinary result by sketching the graphs.

2. Mathematical Model

The flow of Jeffrey fluid is studied in the presence of MHD by considering the diffusion-thermo effect through a porous media. The rectangular coordinates system is oriented in such a way that the x^*-axis is pointing along the plate in the vertical direction and y_2^*-axis is pointing normal to the plate as shown in Figure 1. At the time $t_2^* = 0^+$ the system with the plate and fluid is suppose to be at rest, at the temperature T_∞^* with concentration C_∞^*. However, for the time $t_2^* > 0$, the plate suppose to be moves with exponential velocity $Ue^{at_2^*}$ in its own plane. The plate's temperature as well as concentration of the fluid raised to T_w^* and C_w^* respectively. Magnetic field effect is also considered normally with a constant strength β_0. Energy flux due to concentration gradient is also considered. In view of above assumptions, the Jeffrey fluid flow model with Boussinesq's approximation appears in the following form [3, 13, 28]

$$\frac{\partial u_1(y_2^*, t_2^*)}{\partial t_2^*} = \frac{\nu}{1+\lambda_1}\left(1 + \lambda_2 \frac{\partial}{\partial t_2^*}\right)\frac{\partial^2 u_1(y_2^*, t_2^*)}{\partial {y_2^*}^2} - \frac{\sigma\beta_0^2}{\rho}u_1(y_2^*, t_2^*) - \frac{\mu\phi}{\rho K_1}u_1(y_2^*, t_2^*) + g\beta_{T_1^*}(T_1^* - T_\infty^*) + g\beta_{C_1^*}(C_1^* - C_\infty^*). \tag{1}$$

Thermal Eq. is

$$\rho C_p \frac{\partial T_1^*(y_2^*, t_2^*)}{\partial t_2^*} = -\frac{\partial q_1^*(y_2^*, t_2^*)}{\partial y_2^*} + Q_1 T(T_1^* - T_\infty^*) - \frac{\rho K_T D_m}{DC_S} \frac{\partial J_1^*}{\partial y_2^*}. \tag{2}$$

Fourier's Law states that [29]

$$q_1^*(y_2^*, t_2^*) = -K_2 \frac{\partial T_1^*(y_2^*, t_2^*)}{\partial y_2^*}. \tag{3}$$

Diffusion Eq. is

$$\frac{\partial C_1^*(y_2^*, t_2^*)}{\partial t_2^*} = -\frac{\partial J_1^*(y_2^*, t_2^*)}{\partial y_2^*} - K_3(C_1^* - C_\infty^*). \tag{4}$$

Fick's Law states that, $J_1^*(y_2^*, t_2^*)$ is written as [30]

$$J_1^*(y_2^*, t_2^*) = -D \frac{\partial C_1^*(y_2^*, t_2^*)}{\partial y_2^*}. \tag{5}$$

The initial as well as boundary conditions of the flow problem are [20]

$$\begin{aligned} u_1(y_2^*, t_2^*) &= 0, \\ T_1^*(y_2^*, t_2^*) &= T_\infty^*, \\ C_1^*(y_2^*, t_2^*) &= C_\infty^*, \\ y_2^* &> 0, \\ t_2^* &= 0, \end{aligned} \tag{6}$$

$$\begin{aligned} u_1(0, t_2^*) &= U e^{a_1 t_2^*}, \\ T_1^*(0, t_2^*) &= T_w^*, \\ C_1^*(0, t_2^*) &= C_w^*, \\ a_1 &> 0, t_2^* > 0, \end{aligned} \tag{7}$$

$$\begin{aligned} u_1(y_2^*, t_2^*) &\longrightarrow 0, \\ T_1^*(y_2^*, t_2^*) &\longrightarrow 0, \\ C_1^*(y_2^*, t_2^*) &\longrightarrow 0, \\ y_2^* &\longrightarrow \infty, t_2^* > 0. \end{aligned} \tag{8}$$

The dimensionless form of the flow parameters are

$$\begin{aligned} v &= \frac{u_1}{U}, \\ t &= \frac{U^2 t_2^*}{\nu}, \\ Q &= \frac{Q_1 \nu}{U^2 \rho C_p}, \\ y &= \frac{U y_2^*}{\nu}, \\ \lambda &= \frac{U^2 \lambda_2}{\nu}, \\ J_1 &= \frac{J_1^*}{J}, \\ q_1 &= \frac{q_1^*}{q}, \\ Du &= \frac{\rho K_T D_m J}{UDC_S C_p (T_w - T_\infty)}, \\ Gm &= \frac{g\nu\beta_{C_1^*}(C_w^* - C_\infty^*)}{U^3}, \\ Gr &= \frac{g\nu\beta_{T_1^*}(T_w^* - T_\infty^*)}{U^3}, \\ M &= \frac{\beta_0^2 \sigma \nu}{\rho U^2}, \\ R &= \frac{K_3 \nu}{U^2}, \\ K &= \frac{\mu\phi\nu}{\rho U^2 K_1}, \\ C &= \frac{C_1^* - C_\infty^*}{C_w^* - C_\infty^*}, \\ T &= \frac{T_1^* - T_\infty^*}{T_w^* - T_\infty^*}, \\ a &= \frac{a_1 \nu}{U^2}. \end{aligned} \tag{9}$$

Using non-dimensional variables of equation (9) into equations (1-8), we have

$$\frac{\partial v(y,t)}{\partial t} = (1+\lambda_1)^{-1}\left(1 + \lambda\frac{\partial}{\partial t}\right)\frac{\partial^2 v(y,t)}{\partial y^2} + GrT(y,t) + GmC(y,t) - \left(M + \frac{1}{K}\right)v(y,t),$$

$$\frac{\partial T(y,t)}{\partial t} = -n_2 \frac{\partial q_1(y,t)}{\partial y} + QT(y,t) - Du\frac{\partial J_1}{\partial y} - m_1 \frac{\partial T}{\partial y} = q_1,$$

$$\frac{\partial C(y,t)}{\partial t} = -n_3 \frac{\partial J_1(y,t)}{\partial y} - RC(y,t) - n_1 \frac{\partial C}{\partial y} = J_1,$$

$$v(y,t) = 0,$$

$$T(y,t) = 0,$$

$$C(y,t) = 0, \quad y > 0, t = 0,$$

$$v(0,t) = e^{at},$$

$$T(0,t) = C(0,t) = 1, \quad a > 0, t > 0,$$

$$v(y,t) = T(y,t) = C(y,t) \longrightarrow 0, y \longrightarrow \infty, \tag{10}$$

$$n_2 = \frac{q(T_w - T_\infty)^{-1}}{U\rho C_p},$$

$$n_3 = \left(\frac{(C_w - C_\infty)U}{J}\right)^{-1},$$

$$n_1 = \frac{DU}{(C_w - C_\infty)^{-1} J\nu},$$

$$m_1 = \frac{K_2 U}{(T_w - T_\infty)^{-1} q\nu},$$

where Pr, λ, K, Sc, R, and M represent the Prandtl number, Jeffrey parameter, non-dimensional permeability, Schmidt number, chemical reaction, and magnetic parameter respectively.

3. Generalization of Model

Eq. (10) can be written as

$$\frac{\partial v(y,t)}{\partial t} = \left[\frac{1}{1+\lambda_1} + \frac{\lambda}{1+\lambda_1}\frac{\partial}{\partial t}\right]\frac{\partial^2 v(y,t)}{\partial y^2} - (M + 1/K)(y,t) + \mathrm{Gr}T(y,t) + \mathrm{Gm}C(y,t), \tag{11}$$

Fractional form of Fourier's law [25, 31] is used to generalize Eq. (3) in dimensionless form

$$q_1 = -m_1^{CPC} D_t^{\gamma} \frac{\partial T(y,t)}{\partial y}, \quad 1 \geq \gamma > 0. \tag{12}$$

Fractional form of Fick's Law [25] is used to generalize Eq. (5) in dimensionless form

$$J_1 = -n_1^{CPC} D_t^{\alpha} \frac{\partial C(y,t)}{\partial y}, \quad 1 \geq \alpha > 0. \tag{13}$$

Using equation (12) into (2), and (3) into (3), we get

$$\frac{\partial T(y,t)}{\partial t} = n_2 \frac{\partial}{\partial y}\left(m_1^{\mathrm{CPC}} D_t^{\gamma} \frac{\partial T(y,t)}{\partial y}\right) + QT(y,t) + Du\frac{\partial}{\partial y}\left[n_1^{\mathrm{CPC}} D_t^{\alpha} \frac{\partial C}{\partial y}\right], \tag{14}$$

$$\frac{\partial C(y,t)}{\partial t} = n_3 \frac{\partial}{\partial y}\left[n_1^{CPC} D_t^{\alpha} \frac{\partial C(y,t)}{\partial y}\right] - RC(y,t). \tag{15}$$

Equations (14) and (15) can be written as

$$\frac{\partial T(y,t)}{\partial t} = \frac{1}{\mathrm{Pr}}\,{}^{CPC}D_t^{\gamma} \frac{\partial^2 T(y,t)}{\partial y^2} + QT(y,t) + \mathrm{Dun}_1^{\mathrm{CPC}} D_t^{\alpha} \frac{\partial^2 C}{\partial y^2}, \tag{16}$$

$$\frac{\partial C(y,t)}{\partial t} = \frac{1}{Sc}\,{}^{CPC}D_t^{\alpha} \frac{\partial^2 C(y,t)}{\partial y^2} - RC(y,t). \tag{17}$$

where ${}^{CPC}D_t^{\alpha} f(y,t)$ indicates the CPC fractional derivative of $f(y,t)$ [24] as

$$ {}^{CPC}D_t^{\alpha} f(y,t) = \frac{1}{\Gamma(1-\alpha)} \int_0^t \left(K_1(\alpha) f(y,\tau) + K_0(\alpha) f\prime(y,\tau)(t-\tau) \right)^{-\alpha} d\tau. \tag{18} $$

4. Solution of Problem

The formulated initial and boundary value value problem can be solved by means of the Laplace transform method.

4.1. Concentration Field. (17) be solved via Laplace transform for concentration species as

$$ s\overline{C}(y,s) = Sc^{-1}\left(\frac{k_1(\alpha)}{s} + k_0(\alpha) \right) s^{\alpha}(y,s) - \mathrm{R}\overline{C}(y,s), \tag{19} $$

with

$$ \overline{C}(0,s) = \frac{1}{s}, \quad \overline{C}(y,s) \longrightarrow 0, y \longrightarrow \infty. \tag{20} $$

Put (20) into (19), and result is

$$ \overline{C}(y,s) = \frac{1}{s} e^{-y\sqrt{\frac{(R+s)}{Sc^{-1}(K_1(\alpha)/s + K_0(\alpha))s^{\alpha}}}}. \tag{21} $$

This is complicated to solve analytically. Algorithm [32, 33] is used to derive the numerical result of (21).

4.2. Sherwood Number. The local coefficient of the rate of mass transfer is define in term of Sherwood number, and define by the following relation

$$ Sh = \left. \frac{\partial C}{\partial y} \right|_{y=0} = -L^{-1}\left[\left. \frac{\partial \overline{C}}{\partial y} \right|_{y=0} \right] = L^{-1}\left[\frac{1}{s} \sqrt{\frac{(R+s)}{Sc^{-1}(K_1(\alpha)/s + K_0(\alpha))s^{\alpha}}} \right]. \tag{22} $$

4.3. Temperature Field. (16) be solved via Laplace transform for temperature profile as

$$ s\overline{T}(y,s) = \mathrm{Pr}^{-1}\left(\frac{k_1(\gamma)}{s} + k_0(\gamma) \right) s^{\gamma} \frac{\partial^2 \overline{T}(y,s)}{\partial y^2} + Q\overline{T}(y,s) + n_1 \mathrm{Du}\left(\frac{k_1(\alpha)}{s} + k_0(\alpha) \right) s^{\alpha} \frac{\partial^2 \overline{C}(y,s)}{\partial y^2}, \tag{23} $$

with

$$ \overline{T}(0,s) = \frac{1}{s}, \quad \overline{T}(y,s) \longrightarrow 0, y \longrightarrow \infty. \tag{24} $$

Put (24) into (23), and result is

$$ \overline{T}(y,s) = \frac{1}{s} e^{-y\sqrt{\frac{(s-Q)}{\mathrm{Pr}^{-1}(K_1(\gamma)/s + K_0(\gamma))s^{\gamma}}}} + \frac{n_1 Du(R+s)}{\left(\mathrm{Pr}^{-1}(R+s)/(K_1(\alpha)/s + K_0(\alpha))s^{\alpha} - Sc^{-1}(s-Q)/(K_1(\gamma)/s + K_0(\gamma))s^{\gamma} \right)(k_1(\gamma) + sk_0(\gamma))s^{\gamma}} \times \left(e^{-y\sqrt{\frac{(s-Q)s}{\mathrm{Pr}^{-1}(K_1(\gamma)/s + K_0(\gamma))s^{\gamma}}}} - e^{-y\sqrt{\frac{(R+s)}{Sc^{-1}(K_1(\alpha)/s + K_0(\alpha))s^{\alpha}}}} \right). \tag{25} $$

This is complicated to solve analytically. Algorithm [32, 33] is used to derive the numerical result of (25).

4.4. Nusselt Number. The local coefficient of the rate of heat transfer is define in term of Nusselt number as

$$ Nu = \left. \frac{\partial T}{\partial y} \right|_{y=0} = -L^{-1}\left[\left. \frac{\partial \overline{T}}{\partial y} \right|_{y=0} \right] = L^{-1}\left[\frac{1}{s} \frac{(s-Q)}{\mathrm{Pr}^{-1}(K_1(\gamma)/s + K_0(\gamma))s^{\gamma}} + \frac{n_1 Du(R+s)}{\left(\mathrm{Pr}^{-1}(R+s)/(K_1(\alpha)/s + K_0(\alpha))s^{\alpha} - Sc^{-1}(s-Q)/(K_1(\gamma)/s + K_0(\gamma))s^{\gamma} \right)(k_1(\gamma) + sk_0(\gamma))s^{\gamma}} \times \left(\sqrt{\frac{(s-Q)s}{\mathrm{Pr}^{-1}(K_1(\gamma)/s + K_0(\gamma))s^{\gamma}}} - \sqrt{\frac{(R+s)}{Sc^{-1}(K_1(\alpha)/s + K_0(\alpha))s^{\alpha}}} \right) \right]. \tag{26} $$

4.5. Velocity field. (11) be solved via Laplace transform for velocity field as

$$s\overline{v}(y,t) = \left(1+\lambda_1\right)^{-1}(1+\lambda s)\frac{\partial^2\overline{v}(y,t)}{\partial y^2} - [(M+1/K)\overline{v}(y,t) - \mathrm{Gr}\overline{T}(y,t) - \mathrm{Gm}\overline{C}(y,t)], \tag{27}$$

with

$$\overline{v}(0,s) = (s-a)^{-1}, \quad \overline{v}(y,s) \longrightarrow 0, y \longrightarrow \infty. \tag{28}$$

Put (28) into (27), we get

$$\begin{aligned}\overline{v}(y,s) = {} & \frac{1}{s-a}e^{-y\sqrt{\frac{(s+M+1/K)(1+\lambda_1)}{1+\lambda s}}} \\ & + \frac{\left[\mathrm{Gr}/s + n_1\mathrm{DuGr}(R+s)/\left(\mathrm{Pr}^{-1}(R+s)/\left(K_1(\alpha)/s+K_0(\alpha)\right)s^{\alpha} - \mathrm{Sc}^{-1}(s-Q)/\left(K_1(\gamma)/s+K_0(\gamma)\right)s^{\gamma}\right)\left(k_1(\gamma)+sk_0(\gamma)\right)s^{\gamma}\right]}{\mathrm{Pr}(s-Q)(1+\lambda s)/\left(K_1(\gamma)/s+K_0(\gamma)\right)s^{\gamma}(1+\lambda_1) - (s+M+1/K)} \\ & \cdot\left(e^{-y\sqrt{\frac{(s+M+1/K)(1+\lambda_1)}{1+\lambda s}}} - e^{-y\sqrt{\frac{(s-Q)}{\mathrm{Pr}^{-1}\left(K_1(\gamma)/s+K_0(\gamma)\right)s^{\gamma}}}}\right) + \\ & \frac{\mathrm{Gm}/s - n_1\mathrm{DuGr}(R+s)/\left(\mathrm{Pr}^{-1}(R+s)/\left(K_1(\alpha)/s+K_0(\alpha)\right)s^{\alpha} - \mathrm{Sc}^{-1}(s-Q)/\left(K_1(\gamma)/s+K_0(\gamma)\right)s^{\gamma}\right)\left(k_1(\gamma)+sk_0(\gamma)\right)s^{\gamma}}{\mathrm{Sc}(R+s)(1+\lambda s)/\left(K_1(\alpha)/s+K_0(\alpha)\right)s^{\alpha}(1+\lambda_1) - (s+M+1/K)} \\ & \cdot\left(e^{-y\sqrt{\frac{(s+M+1/K)(1+\lambda_1)}{1+\lambda s}}} - e^{-y\sqrt{\frac{(R+s)}{\mathrm{Sc}^{-1}\left(K_1(\alpha)/s+K_0(\alpha)\right)s^{\alpha}}}}\right).\end{aligned} \tag{29}$$

This is complicated to solve analytically. Algorithm [32, 33] is used to derive the numerical result of (29).

4.6. Skin Friction. The expression of skin friction is define by using (29) as

$$\begin{aligned}\tau = \frac{\partial u}{\partial y}|_{y=0} = -L^{-1}\left[\frac{\partial\overline{u}}{\partial y}|_{y=0}\right] = L^{-1}\Bigg[& \frac{1}{s-a}\sqrt{\frac{(s+M+1/K)(1+\lambda_1)}{1+\lambda s}} \\ & + \frac{\mathrm{Gr}/s + n_1\mathrm{DuGr}(R+s)/\left(\mathrm{Pr}^{-1}(R+s)/\left(K_1(\alpha)/s+K_0(\alpha)\right)s^{\alpha} - \mathrm{Sc}^{-1}(s-Q)/\left(K_1(\gamma)/s+K_0(\gamma)\right)s^{\gamma}\right)\left(k_1(\gamma)+sk_0(\gamma)\right)s^{\gamma}}{\mathrm{Pr}(s-Q)(1+\lambda s)/\left(K_1(\gamma)/s+K_0(\gamma)\right)s^{\gamma}(1+\lambda_1) - (s+M+1/K)} \\ & \times\left(\sqrt{\frac{(s+M+1/K)(1+\lambda_1)}{1+\lambda s}} - \sqrt{\frac{(s-Q)}{\mathrm{Pr}^{-1}\left(K_1(\gamma)/s+K_0(\gamma)\right)s^{\gamma}}}\right)\end{aligned}$$

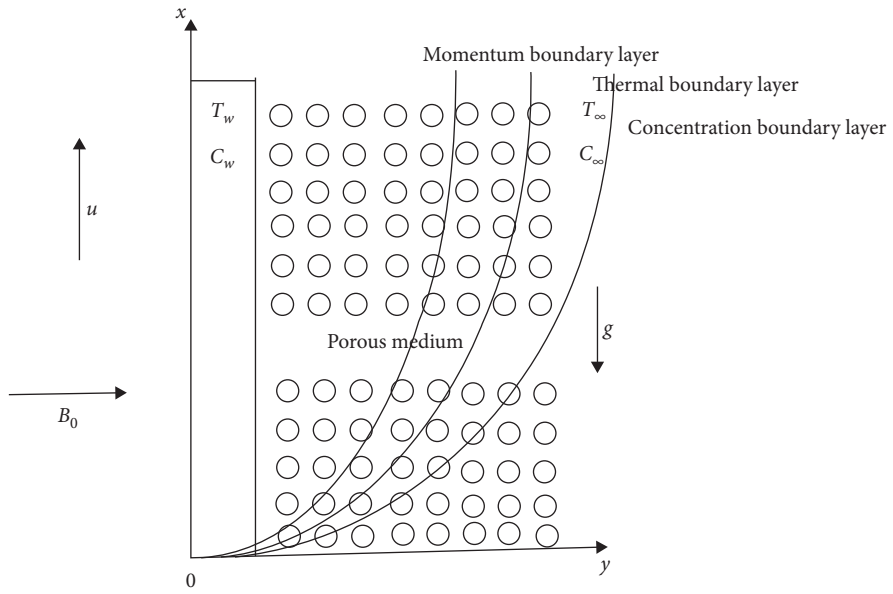

Figure 1: Physical model.

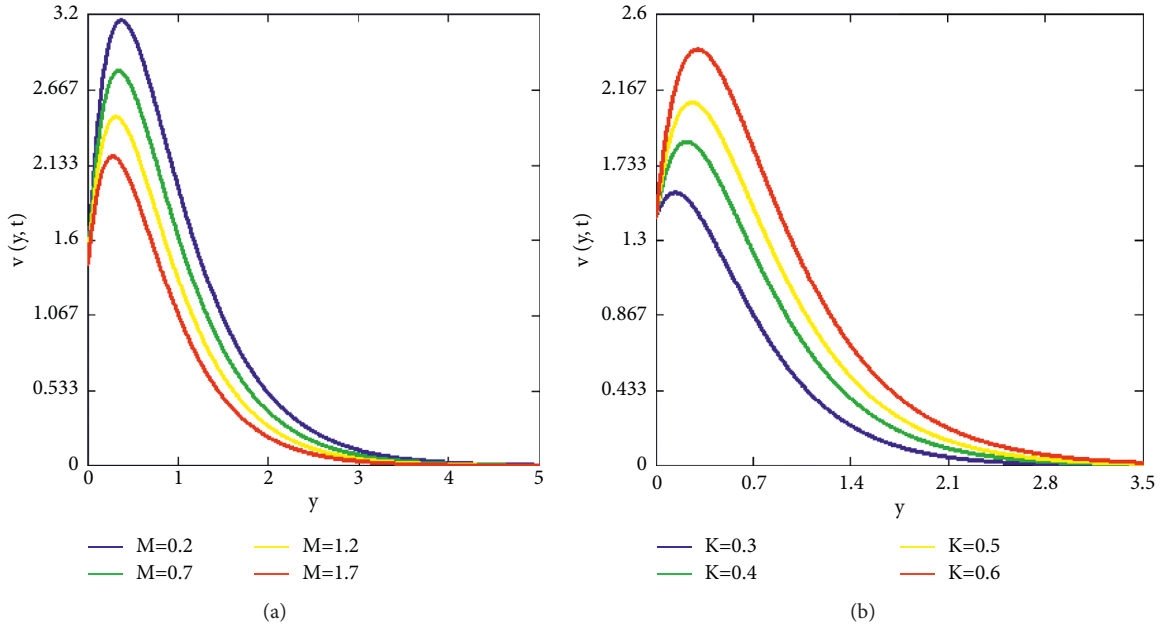

Figure 2: (a) Velocity profile $v(y,t)$ for parameter M at $R=3.2$, $Q=4$, Gr = 14, Gm = 8, Du = 0.4, Sc = 2.5, Pr = 6, and $K=2$. (b) Velocity profile $v(y,t)$ for parameter K at $R=3.2$, $Q=4$, Gr = 14, Gm = 8, $M=4$, Sc = 2.5, Pr = 6, and Du = 0.4.

$$+\frac{\mathrm{Gm}/s-n_1\mathrm{DuGr}\,(R+s)/\left(\mathrm{Pr}^{-1}\,(R+s)/\left(K_1\,(\alpha)/s+K_0\,(\alpha)\right)s^{\alpha}-\mathrm{Sc}^{-1}\,(s-Q)/\left(K_1\,(\gamma)/s+K_0\,(\gamma)\right)s^{\gamma}\right)\left(k_1\,(\gamma)+sk_0\,(\gamma)\right)s^{\gamma}}{\mathrm{Sc}\,(R+s)\,(1+\lambda s)/\left(K_1\,(\alpha)/s+K_0\,(\alpha)\right)s^{\alpha}\left(1+\lambda_1\right)-(s+M+1/K)}$$
$$\times\left(\sqrt{\frac{(s+M+1/K)\,(1+\lambda_1)}{1+\lambda s}}-\sqrt{\frac{(R+s)}{\mathrm{Sc}^{-1}\left(K_1\,(\alpha)/s+K_0\,(\alpha)\right)s^{\alpha}}}\right)\Bigg]. \tag{30}$$

5. Results and Discussion

In this article the diffusion-thermo effect is investigated for the magnetohydrodynamics (MHD) flow of Jeffrey's fractional fluid past an exponentially accelerated vertical plate with generalized thermal and mass transports through a porous medium. The semi-analytical results for the concentration, temperature, and velocity fields are obtained.

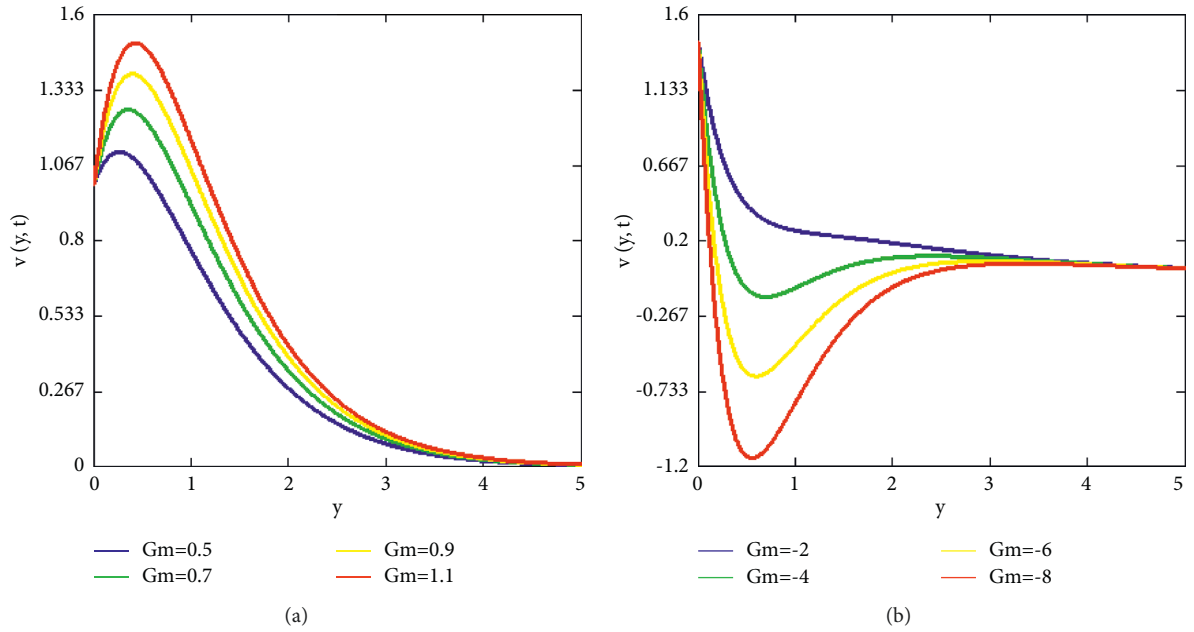

Figure 3: (a) Velocity profile $v(y,t)$ for parameter Gm at $R=3.2$, $Q=4$, Gr = 14, Du = 0.4, $M=4$, Sc = 2.5, Pr = 6, and $K=2$. (b) Velocity profile $v(y,t)$ for parameter Gm at $R=3.2$, $Q=4$, Gr = 14, Du = 0.4, $M=4$, Sc = 2.5, Pr = 6, and $K=2$.

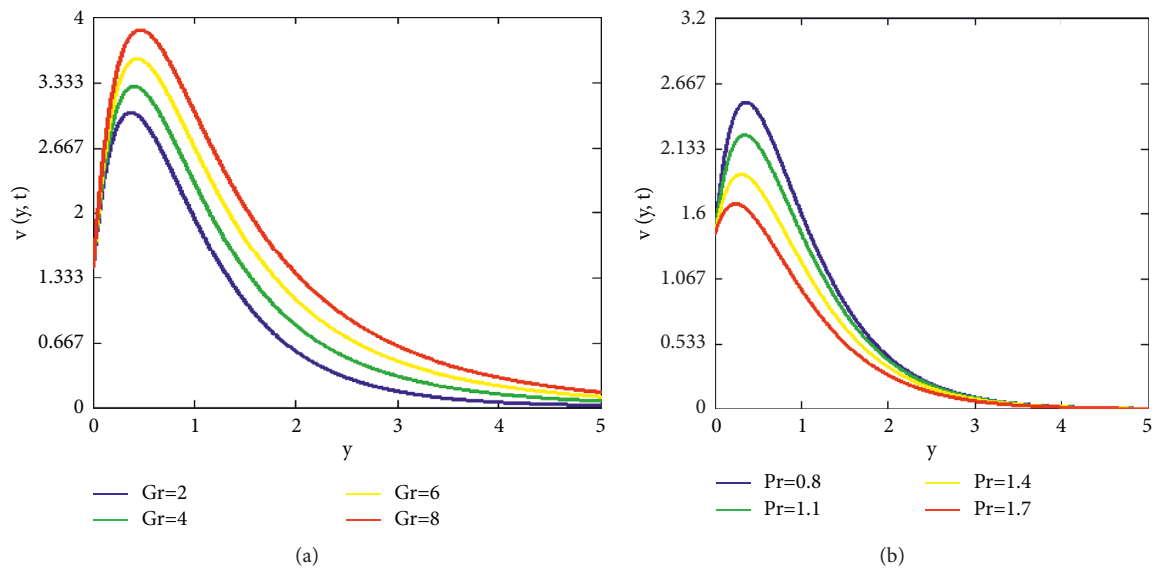

Figure 4: (a) Velocity profile $v(y,t)$ for parameter Gr at $R=3.2$, $Q=4$, Gm = 8, $M=4$, Sc = 2.5, Pr = 6, and $K=2$. (b) Velocity profile $v(y,t)$ for parameter Pr at $R=3.2$, $Q=4$, Gr = 14, Gm = 8, $M=4$, Sc = 2.5, Du = 0.4, and $K=2$.

Moreover to see the physical effect of involved parameters, the concentration, temperature, and velocity fields are postured by some graphs.

Velocity profile is sketched in the Figure 2(a) to twilight the influence magnetic field over the fluid velocity and it is observed that fluid slows down for greater values of M. In the presence of magnetic field a retarding force is created which oppose the fluid motion as depicted in Figure 2(a). The effect of porosity parameter K on fluid flow is defected in Figure 2(b) and it is noted that the fluid motion enhance with increasing value of K. The larger value of K refers to the less Darcy resistance to the flow that is why flow speeds up with increasing value of K. The influence of mass Gm on fluid velocity $v(y,t)$ is illustrate in Figures 3(a) and 3(b). It is noted that fluid motion increases as values of Gm increasing. Physically higher values of Gm refers the higher concentration gradients and greater the buoyancy force and more current in flow domain so velocity increases. Figure 4(a) represent the result of Gr on fluid velocity $v(y,t)$. The fluid motion rises up with maximizing the values of Gr, and it represents the more impact of thermal buoyancy force as compare to the viscous effect. Therefore maximizing the values of Gr refers the higher temperature gradient due to which

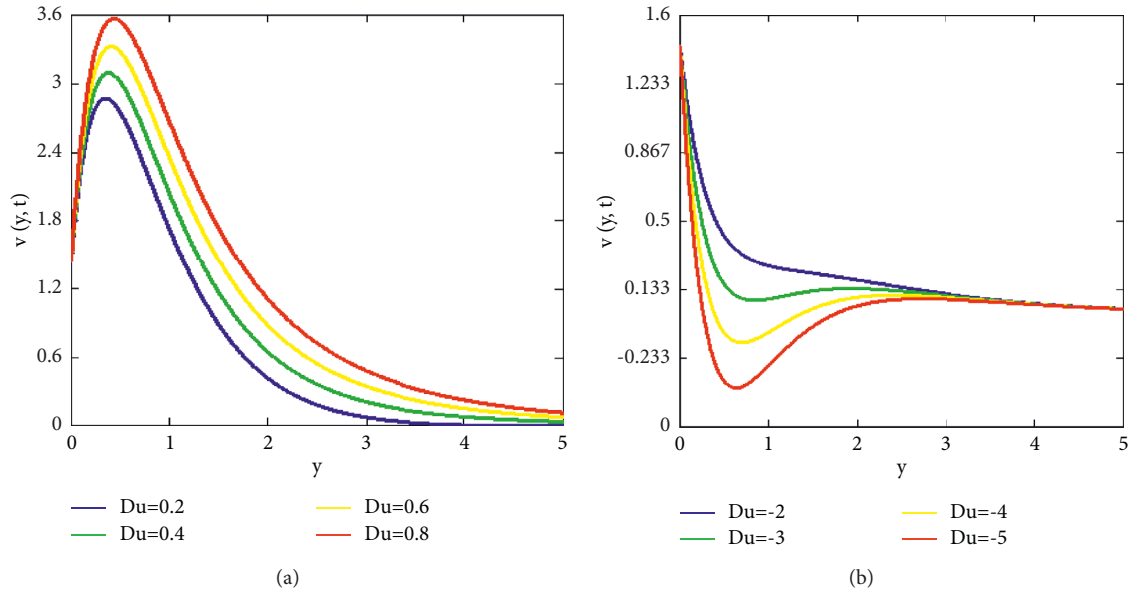

Figure 5: (a) Velocity profile $v(y,t)$ for parameter Du at $R=3.2$, $Q=4$, Gr = 14, Gm = 8, $M=4$, Sc = 2.5, Pr = 6, and $K=2$. (b) Velocity profile $v(y,t)$ for parameter Du at $R=3.2$, $Q=4$, Gr = 14, Gm = 8, $M=4$, Sc = 2.5, Pr = 6, and $K=2$.

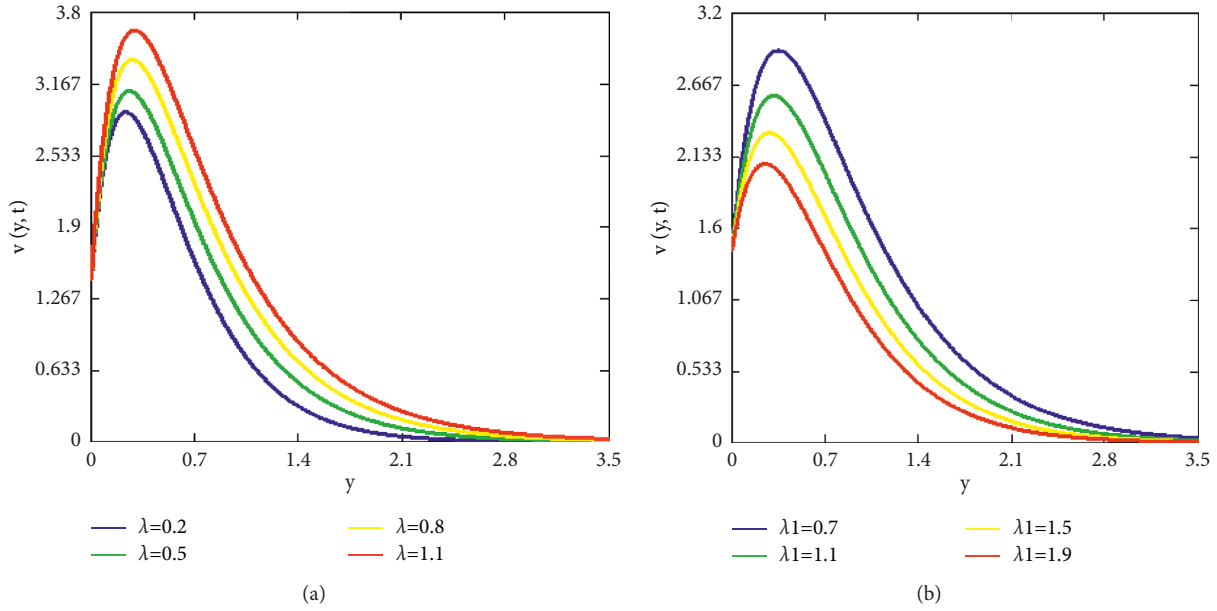

Figure 6: (a) Velocity profile $v(y,t)$ for heat generation parameter λ at $R=3.2$, Q = 4, Gr = 14, Gm = 8, $M=4$, Sc = 2.5, Pr = 6, and $K=2$. (b) Velocity profile $v(y,t)$ for chemical reaction parameter λ_1 at $R=3.2$, $Q=4$, Gr = 14, Gm = 8, $M=4$, Sc = 2.5, Pr = 6, and $K=2$.

velocity field rises. The impact of Pr for velocity field is presented in Figure 4(b).

The diffusion-thermo or Dufour effect (Du) over the velocity field are discussed in the Figures 5(a) and 5(b). An enhancing flow pattern is observed due to the increasing variations of the Du. The concentration gradient give a contribute to the temperature gradient which creates an additional energy flux in the flow domain. Therefore an increasing value of the Du refer to the more energy flux which generates the more flow current that is why the flow speeds up with increasing value of Du. Moreover the negative values refer to the opposite direction of the additional energy flux therefore more negativity of Du generates the more opposite flow current in the flow domain.

Figures 6(a) and 6(b) are drawn to see impact of Jeffrey parameters λ and λ_1 over velocity field $v(y,t)$ respectively. As parameter λ refer to the viscosity of the fluid therefore fluid velocity falls due to the increasing value of λ and the parameter λ_1 refers to the elasticity of the fluid material so fluid speed up with increasing value λ_1. The influence of heat generation on $v(y,t)$ is reported in Figure 7(a). An increasing value of R decreases the fluid velocity as shown in Figure 7(b). The impact of Sc on $v(y,t)$ is illustrate in Figure

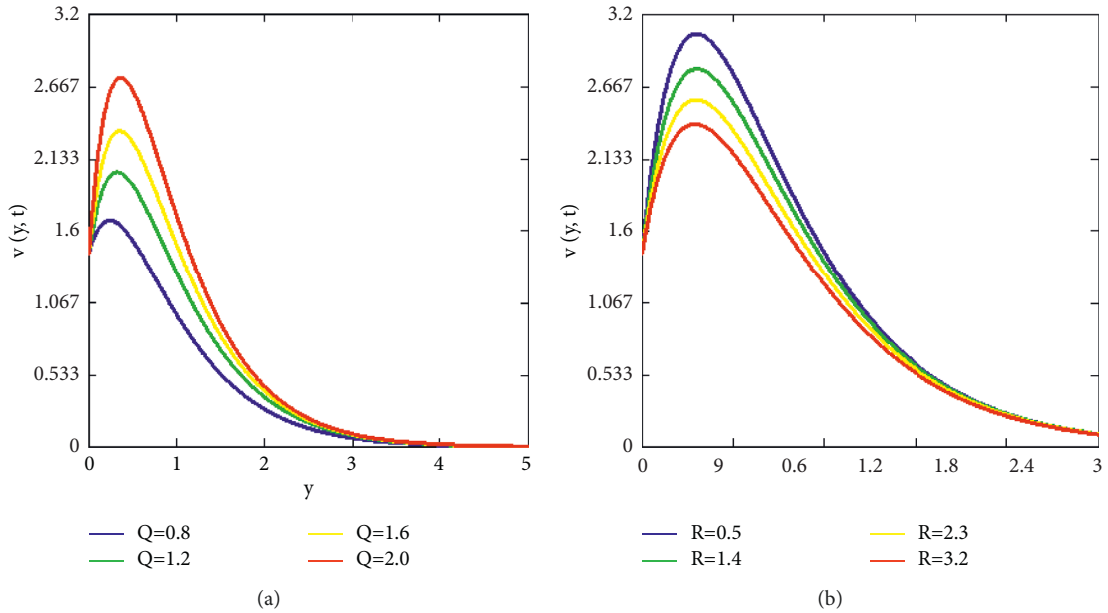

FIGURE 7: (a) Velocity profile $v(y,t)$ for heat generation parameter Q at $R = 3.2$, Du = 0.4, Gr = 14, Gm = 8, $M = 4$, Sc = 2.5, Pr = 6, and $K = 2$. (b) Velocity profile $v(y,t)$ for chemical reaction parameter R at $Q = 4$, Du = 0.4, Gr = 14, Gm = 8, $M = 4$, Sc = 2.5, Pr = 6, and $K = 2$.

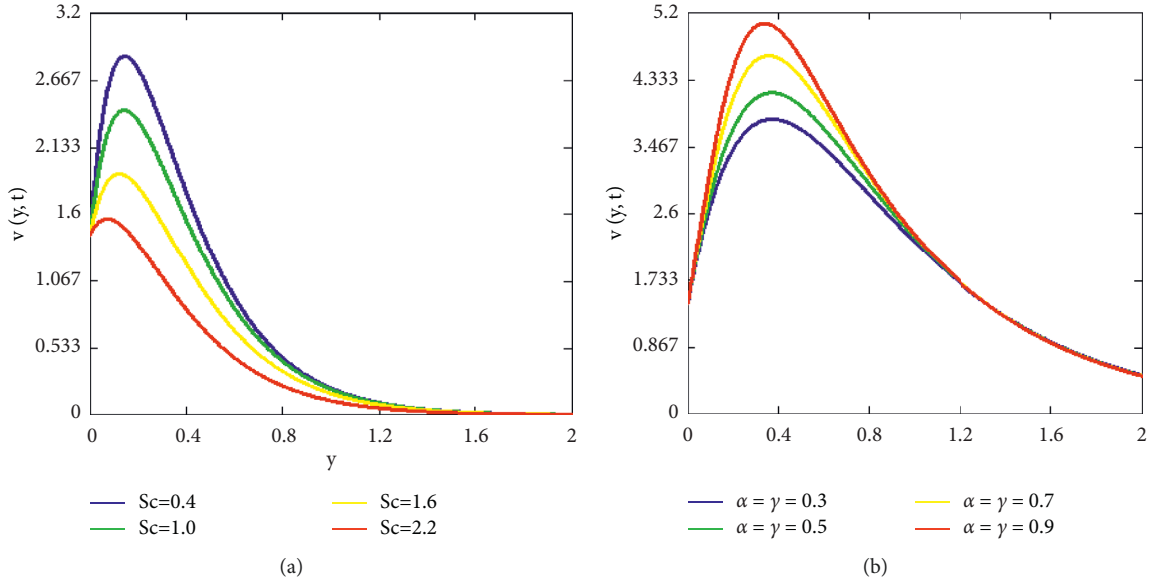

FIGURE 8: Velocity profile $v(y,t)$ for parameter Sc at $R = 3.2$, $Q = 4$, Gr = 14, Gm = 8, $M = 4$, Du = 0.4, Pr = 6, and $K = 2$. (b) Velocity profile $v(y,t)$ for fractional parameters at $Q = 4$, Du = 0.4, Gr = 14, Gm = 8, M = 4, R = 3.2, Du = 0.4, Pr = 6, and $K = 2$.

8(a). Here, maximizing the values of Sc slow down the fluid motion due to decay of molecular diffusion. It is analyzed that motion of fluid increases with raising values of $\alpha = \gamma$ as depicted in Figure 8(b). The graphical behavior of Du, Pr, Q, and t on $T(y,t)$ are shown in Figures 9(a), 9(b), 10(a) as well as 10(b) respectively. Figures illustrate that temperature reduces by exceeding the values of Du, and Pr, and temperature increases by exceeding the values of Q and t. The impacts of Schmidt number Sc as well as chemical reaction R on $C(y,t)$ are present in Figures 11(a) as well as 11(b) respectively. Figures 12(a) and 12(b) represent the comparison of velocity and temperature distribution of present work with Naseem [20] respectively. If we take fractional parameters $\alpha = \gamma \longrightarrow 1, = \lambda = \lambda_1 = M = \text{Gm} = \text{Du} = Q = 0$, $1/K \longrightarrow 0, 1/\gamma \longrightarrow 0$ and $f(t) = e^{at_2^*}$ in Naseem [28], the velocity fields are identical that shows the validity of this present work. Moreover the comparison of present work with other fractional derivatives Caputo and Caputo Fabrizio used in Nazar et al. [34] and Nadeem et al. [35] respectively in the absence of K, Q, Gm, R, Du are shown in Figure 12(c). If we put $\alpha = 1$ the fluid curves are identical as shown in Figure 12(d). From the figures, it is concluded that Jeffrey fluid with CPC fractional derivative is the best choice to enhance the fluid motion. Figures 13(a) and 13(b)

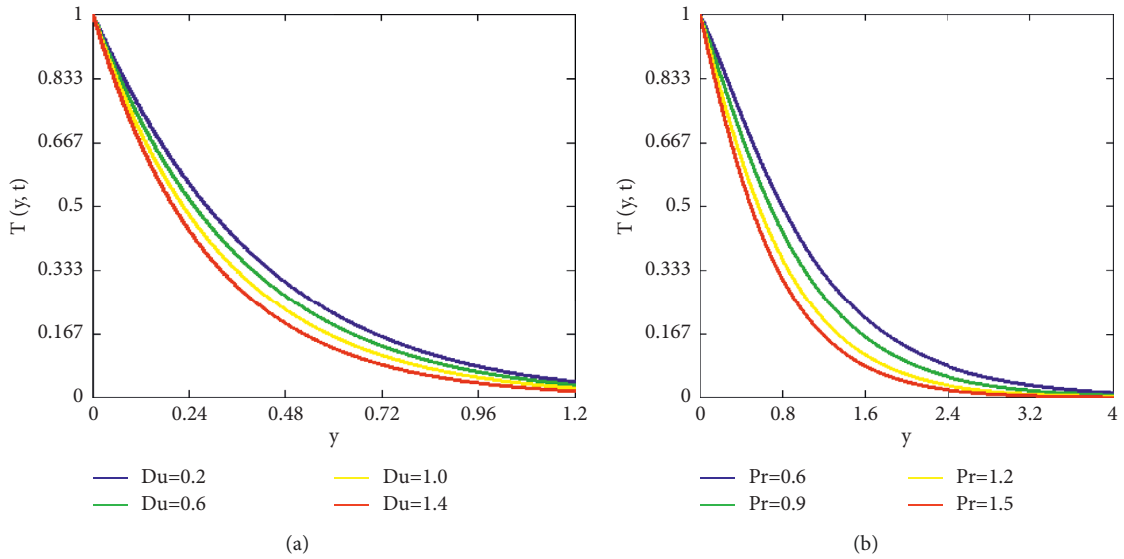

Figure 9: (a) Temperature profile $T(y,t)$ for parameter Du. (b) Temperature profile $T(y,t)$ for Pr.

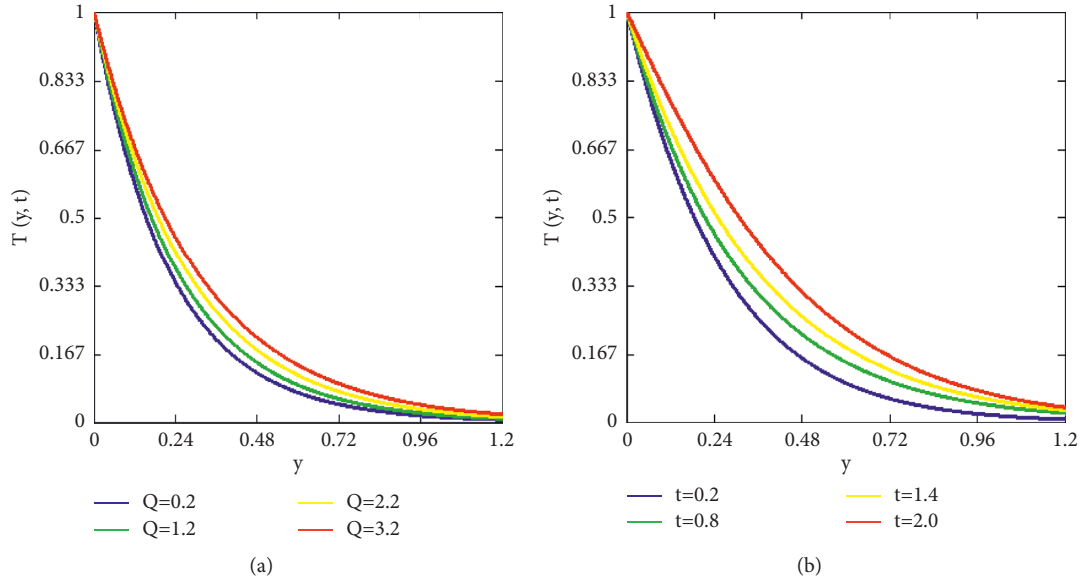

Figure 10: Temperature profile $T(y,t)$ for parameter Q. (b) Temperature profile $T(y,t)$ for t.

represent the authenticity of inversion algorithms for temperature and concentration distributions. The velocity distributions overlap which shows the authenticity of inversion algorithms as presented in Figure 14. Skin friction, rate of heat and mass transfer can be enhanced by increasing the values of fractional parameter and presented in table 1.

- With decreasing fractional parameter values, the velocity distribution slows down.
- Thermal buoyancy forces accelerate the fluid velocity.
- Fluid velocity reduces as Schmidt number Sc, chemical reaction R, and magnetic parameter M rises.
- The fluid velocity increased for larger values of Jeffrey parameter as well as fractional parameter.
- The temperature distribution increases by the smaller values of Prandtl number Pr.

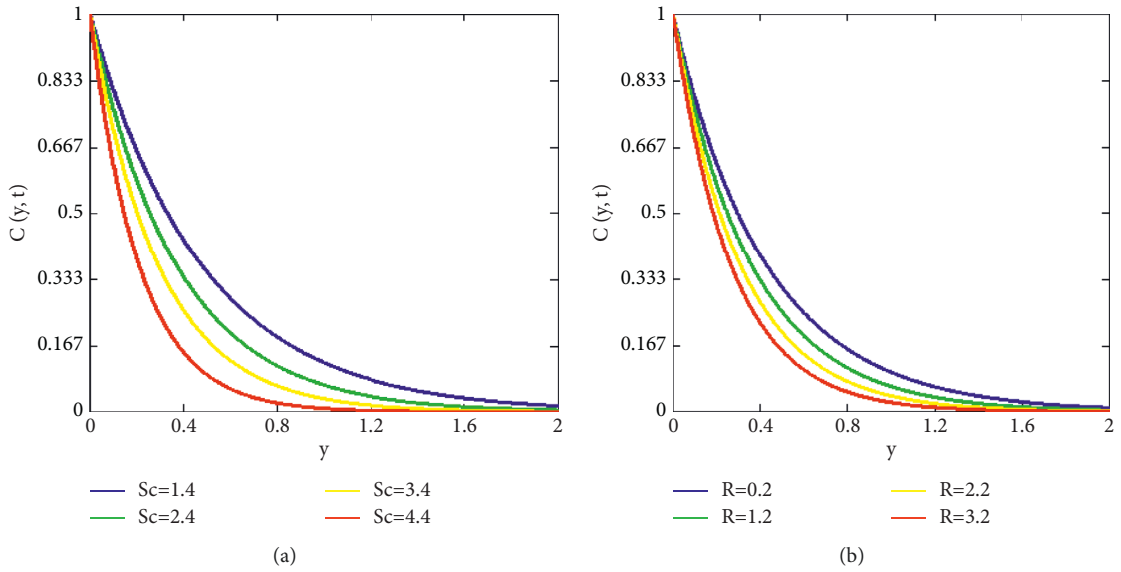

Figure 11: (a) Concentration profile $C(y,t)$ for parameter Sc. (b) Concentration profile $C(y,t)$ for parameter R.

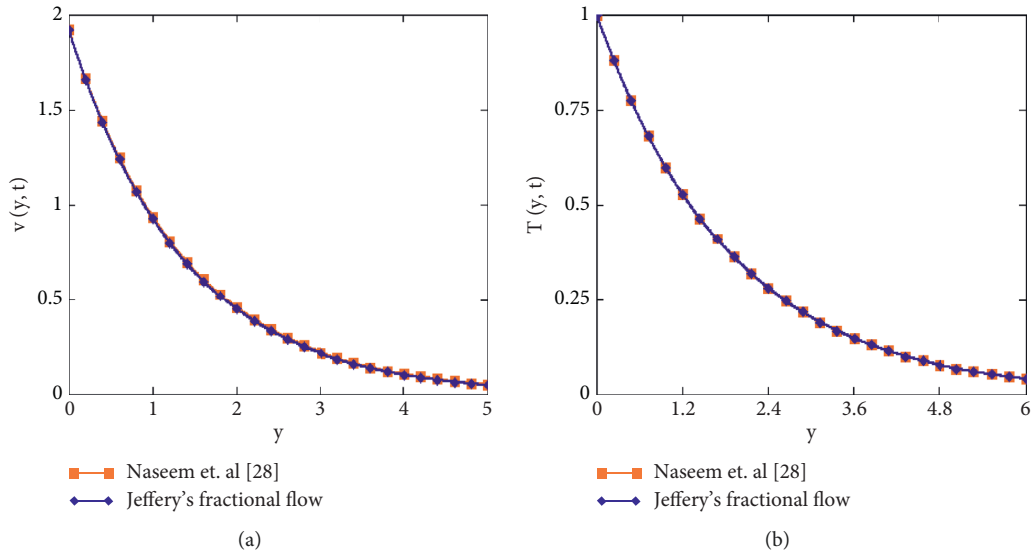

Figure 12: Continued.

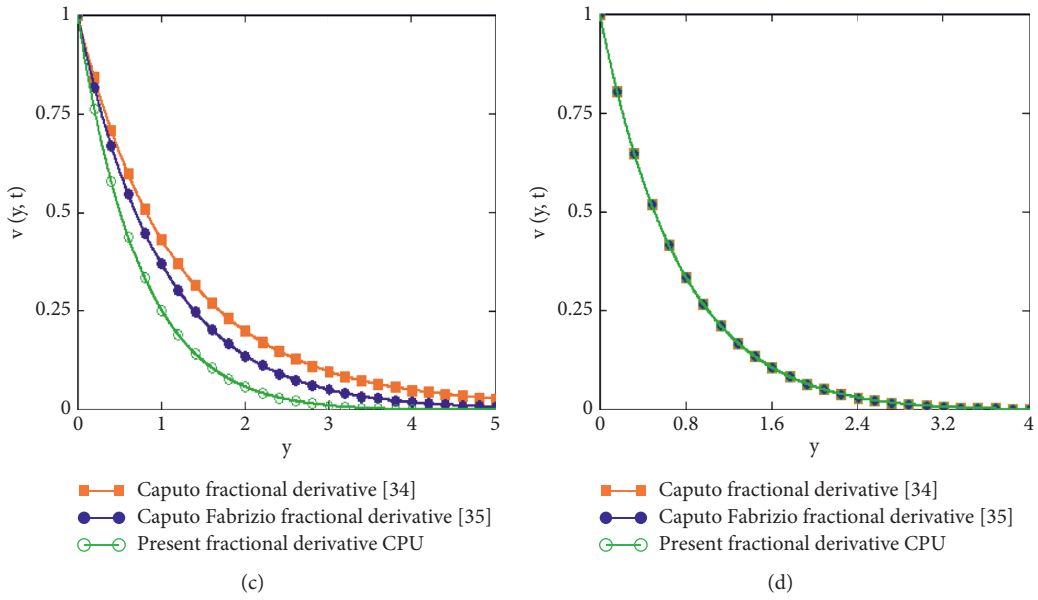

Figure 12: (a) Velocity distribution for comparison of our work with Naseem [28] as $\alpha = \gamma \to 0, \lambda = \lambda = M = Gm = Du = Q = 0, 1/K \to 0, 1/\gamma \to 0$. (b) Temperature for comparison of our work with Naseem [28] as $\alpha = \gamma \to 1$, $Gm = Du = Q = 0$. (c) Comparisons between different fractional derivatives $\alpha = 0.5$ (d) Comparisons between different fractional derivatives $\alpha \to 1$.

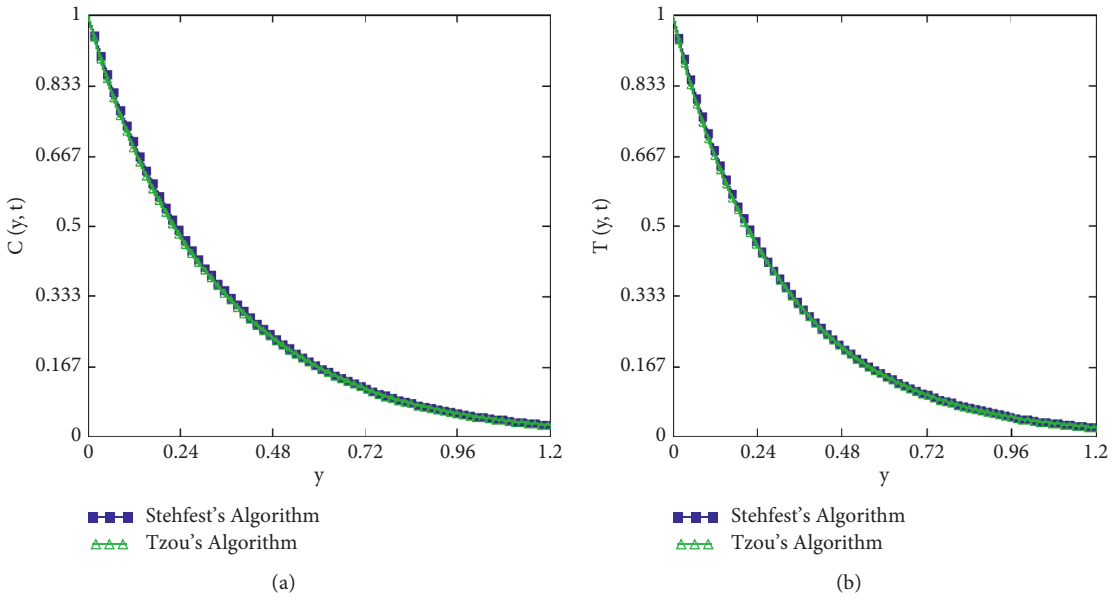

Figure 13: (a) Concentration obtained by Stehfest's and Tzou's algorithms. (b) Temperature obtained by Stehfest's and Tzou's algorithms.

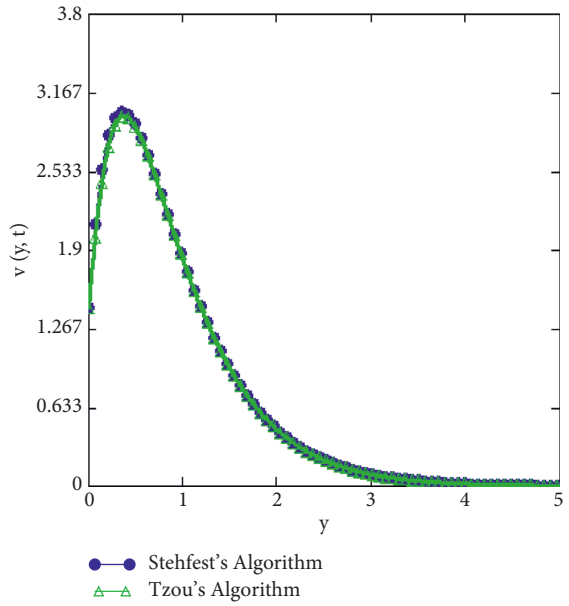

Figure 14: Velocity obtained by Stehfest's and Tzou's algorithms.

Table 1: Effect of α on skin friction, Nusselt number, and Sherwood number.

Fractional Parameter	skin friction	Nusselt number	Sherwood number
0.1	1.458 939 71	1.363 328 25	1.293 234 41
0.2	1.469 733 54	1.376 590 53	1.306 809 85
0.3	1.480 812 22	1.389 919 45	1.320 272 42
0.4	1.492 212 41	1.403 398 90	1.333 699 19
0.5	1.503 987 04	1.417 120 90	1.347 160 76
0.6	1.516 206 97	1.431 188 59	1.360 720 51
0.7	1.528 970 61	1.445 719 09	1.374 431 12
0.8	1.542 413 61	1.460 842 28	1.388 325 48
0.9	1.556 732 82	1.476 693 47	1.402 406 85
0.99	1.572 220 17	1.493 394 87	1.416 634 77

•The concentration distribution decreases for greater values of Schmidt number Sc.

• The concentration distribution decreases by exceeding the values of chemical reaction R.

6. Conclusions

The Magnetohydrodynamics flow model of Jeffrey's fractional fluid model has been considered with the effect of magnetic field in the porous regime. Heat generation, and radiation are also consider with effect of chemical reaction in the flow domain. This flow model is solved analytically and results for velocity, temperature, and concentration fields are constructed by using Laplace transform. Further different graphs of optimising fields are plotted to highlight the influence parameters. The key outcomes of this flow model are:

Nomenclature

v: : fluid velocity, $[ms^{-1}]Sr$: Soret number
Gr: : Thermal Grashof number, $[\beta T_w]Gm$: Mass Grashof number, $[\beta T_w]Nu$: Nusselt number
Sc: : Schmidt number
λ: : Jeffrey parameter
g: acceleration due to gravity, $[ms^{-2}]C_p$: Specific heat at a constant pressure, $[jkg^{-1}K^{-1}]T$: Temperature of fluid, $[K]T_w$: Fluid temperature at plate, $[K]T_\infty$: Fluid temperature far away from the plate, $[K]C$: Concentration of fluid, $[kgm^{-3}]C_w$: Concentration level at plate, $[kgm^{-3}]C_\infty$: Concentration of the fluid far away from the plate, $[kgm^{-3}]s$: Laplace transform parameter
ρ: Fluid density, $[kgm^{-3}]\alpha$: Fractional parameter
ν: Kinematic viscosity, $[m^2s^{-1}]\beta_T$: Volumetric Coefficient of thermal expansion, $[K^{-1}]\beta_C$: Volumetric Coefficient of mass expansion, $[m^3kg^{-1}]$.

Data Availability

The data used to support the findings of this study are included within the article.

Additional Points

With decreasing fractional parameter values, the velocity distribution slows down. Thermal buoyancy forces accelerate the fluid velocity. Fluid velocity reduces as Schmidt number Sc, chemical reaction R, and magnetic parameter M rise. The fluid velocity increased for larger values of Jeffrey parameter as well as fractional parameter. The temperature distribution increases by the smaller values of Prandtl

number Pr. The concentration distribution decreases for greater values of Schmidt number Sc. The concentration distribution decreases by exceeding the values of the chemical reaction R.

Conflicts of Interest

The authors declare that they have no conflicts of interest.

References

[1] N. A. Mohd Zin, A. Q. Mohamad, I. Khan, and S. Shafie, "Porosity effect on unsteady MHD free convection flow of Jeffrey fluid past an oscillating vertical plate with ramped wall temperature," *Malaysian Journal of Fundamental and Applied Sciences*, vol. 13, pp. 49–59, 2017.

[2] S. Bajwa, S. Ullah, I. Khan, and M. Fayz-Al-Asad, "Transient flow of Jeffrey fluid over a permeable wall," *Mathematical Problems in Engineering*, vol. 2021, pp. 1–9, Article ID 9999949, 2021.

[3] M. Asgir, A. A. Zafar, A. M. Alsharif, M. B. Riaz, and M. Abbas, "Special function form exact solutions for Jeffery fluid: an application of power law kernel," *Advances in Difference Equations*, pp. 1–18, 2021.

[4] K. Das, "Influence of slip and heat transfer on MHD peristaltic flow of a Jeffrey fluid in an inclined asymmetric porous channel," *Indian Journal of Mathematics*, vol. 54, pp. 19–45, 2012.

[5] M. Qasim, "Heat and mass transfer in a Jeffrey fluid over a stretching sheet with heat source/sink," *Alexandria Engineering Journal*, vol. 52, no. 4, pp. 571–575, 2013.

[6] F. Ali, M. Khan, and M. Gohar, "Magnetohydrodynamic fluctuating free convection flow of Second-grade fluid flow in a porous medium," *Mathematical Problems in Engineering*, vol. 2021, pp. 1–13, 2021.

[7] N. A. Shah, M. Areshi, J. D. Chung, and K. Nonlaopon, "The new semianalytical technique for the solution of fractional-order Navier-Stokes equation," *Journal of Function Spaces*, vol. 2021, pp. 1–13, 2021.

[8] K. V. Chandra, "Laplace transform solution of unsteady MHD Jeffrey fluid flow past vertically inclined porus plate," *Frontiers in Heat and Mass Transfer*, pp. 1–6, 2021.

[9] M. Jamil and A. Haleem, "MHD fractionalized Jeffrey fluid over an accelerated slipping porous plate," *Nonlinear Engineering*, vol. 9, no. 1, pp. 273–289, 2020.

[10] K. A. Abro, I. A. Abro, S. M. Almani, and I. Khan, "On the thermal analysis of magnetohydrodynamic Jeffery fluid via modern non integer order derivative," *Journal of King Saud University Science*, vol. 31, no. 4, pp. 973–979, 2019.

[11] A. Atangana, A. Akgul, and K. M. Owolabi, "Analysis of fractal fractional differential equations," *Alexandria Engineering Journal*, vol. 59, pp. 1–18, 2020.

[12] A. Atangana and J. F. Gómez-Aguilar, "Numerical approximation of Riemann-Liouville definition of fractional derivative: from Riemann-Liouville to Atangana-Baleanu," *Numerical Methods for Partial Differential Equations*, vol. 34, no. 5, pp. 1502–1523, 2018.

[13] J. Ahmad, F. Ali, S. Murtaza, and I. Khan, "Caputo time fractional model based on generalized Fourier's and Fick's laws for Jeffrey Nano fluid: applications in automobiles," *Mathematical Problems in Engineering*, vol. 2021, pp. 1–12, Article ID 4611656, 2021.

[14] I. Siddique, S. Ayaz, and F. Jarad, "Dufour effect on transient MHD double convection flow of fractionalized second-grade fluid with caputo-fabrizio derivative," *Complexity*, vol. 2021, pp. 1–21, 2021.

[15] N. Sandeep and C. Sulochana, "Momentum and heat transfer behaviour of Jeffrey, Maxwell and Oldroyd-B nanofluids past a stretching surface with non-uniform heat source/sink," *Ain Shams Engineering Journal*, vol. 9, no. 4, pp. 517–524, 2018.

[16] S. Saleem, M. M. Al-Qarni, S. Nadeem, and N. Sandeep, "Convective heat and mass transfer in magneto Jeffrey fluid flow on a rotating cone with heat source and chemical reaction," *Communications in Theoretical Physics*, vol. 70, no. 5, p. 534, 2018.

[17] C. Sulochana, S. R. Aparna, and N. Sandeep, "Heat and mass transfer of magnetohydrodynamic Casson fluid flow over a wedge with thermal radiation and chemical reaction," *Heat Transfer*, vol. 50, no. 4, pp. 3704–3721, 2021.

[18] N. Acharya, R. Bag, and P. K. Kundu, "Unsteady bioconvective squeezing flow with higher-order chemical reaction and second-order slip effects," *Heat Transfer*, vol. 50, no. 6, pp. 5538–5562, 2021.

[19] N. Acharya, H. Mondal, and P. K. Kundu, "Spectral approach to study the entropy generation of radiative mixed convective couple stress fluid flow over a permeable stretching cylinder," vol. 235, pp. 2692–2704, 2021.

[20] N. Acharya, S. Maity, and P. K. Kundu, "Differential transformed approach of unsteady chemically reactive nanofluid flow over a bidirectional stretched surface in presence of magnetic field," *Heat Transfer*, vol. 49, no. 6, pp. 3917–3942, 2020.

[21] A. Riaz, S. Nadeem, R. Ellahi, and N. S. Akbar, "The influence of wall flexibility on unsteady peristaltic flow of Prandtl fluid in a three dimensional rectangular duct," *Applied Mathematics and Computation*, vol. 241, pp. 389–400, 2014.

[22] A. Riaz, R. Ellahi, and S. M. Sait, "Role of hybrid nanoparticles in thermal performance of peristaltic flow of Eyring-Powell fluid model," *Journal of Thermal Analysis and Calorimetry*, vol. 143, no. 2, pp. 1021–1035, 2021.

[23] Yuri-Luchko, "Book on fractional integrals and derivatives: "true" versus "false," *Mathematics*, pp. 1–283, 2021.

[24] D. Baleanu, A. Fernandez, and A. Akgül, "On a fractional operator combining proportional and classical differintegrals," *Mathematics*, vol. 8, no. 3, p. 360, 2020.

[25] Y. M. Chu, M. Ahmad, M. I. Asjad, and D. Baleanu, "Fractional model of Second grade fluid induced by generalized thermal and molecular fluxes with constant proportional Caputo," *Thermal Science*, vol. 25, pp. 1–6, 2021.

[26] I. Siddique and A. Akgul, "Analysis of blood liquor model via nonlocal and singular constant proportional Caputo hybrid differential operator," *Mathematical Methods in the Applied Sciences*, pp. 1–17, 2021.

[27] D. khan, P. Kumam, and W. Watthayu, "A novel comparative case study of entropy generation for natural convection flow of proportional.Caputo hybrid and Atangana baleanu fractional derivative," *Scientific Reports*, vol. 11, pp. 1–11, 2021.

[28] A. Naseem, "General solution of Casson fluid past a vertical plate subject to the time dependent velocity with constant wall temperature," *Open Journal of Mathematical Analysis*, vol. 2(2018), no. 1, pp. 47–65, 2018.

[29] G. B. Arfken, D. F. Griffing, D. C. Kelly, and J. Priest, "Instructional aids to accompany university physics," *International Edition University Physics*, pp. 1–905, 1984.

[30] D. R. Poirier and G. H. Geifer, *Transport Phenomena in Materials Processing*, pp. 1–660, Springer, Berlin/Heidelberg, Germany, 2016.

[31] J. Hristov, "Transient heat diffusion with a non-singular fading memory from the cattaneo constitutive equation with Jeffrey's kernel to the Caputo-fabrizio time fractional derivative," *Thermal Science*, vol. 20, pp. 557–562, 2016.

[32] D. Y. Tzou, *Macro to Microscale Heat Transfer, the Lagging Behavior*, pp. 01–339, Taylor & Francis, Washington, District of Columbia, 1997.

[33] H. Stehfest, "Algorithm 368: numerical inversion of Laplace transforms [D5]," *Communications of the ACM*, vol. 13, no. 1, pp. 47–49, 1970.

[34] M. Nazar, M. Ahmad, M. A. Imran, and N. A. Shah, "Double convection of heat and mass transfer flow of mhd generalized Second grade fluid over an exponentially accelerated infinite vertical plate with heat absorption," *Journal of Mathematical Analysis*, vol. 8, pp. 28–44, 2017.

[35] N. A. Sheikh, F. Ali, I. Khan, and M. Saqib, "A modern approach of Caputo-Fabrizio time-fractional derivative to MHD free convection flow of generalized second-grade fluid in a porous medium," *Neural Computing & Applications*, vol. 30, no. 6, pp. 1865–1875, 2018.